Plasma Control for NCSX and Development of Equilibrium Reconstruction for Stellarators

N. Pomphrey,[1] L.L. Lao,[2] E.A. Lazarus,[3] M.C. Zarnstorff,[1] J.D. Hanson,[4] S.P. Hirshman,[3] S.R. Hudson,[1] S.F. Knowlton,[4] L-P. Ku,[1] D.C. McCune,[1] D. Mikkelsen,[1] D.A. Monticello,[1] and A.H. Reiman[1]

[1]Princeton Plasma Physics Laboratory, Princeton, New Jersey, USA
[2]General Atomics, San Diego, California, USA
[3]Oak Ridge National Laboratory, Oak Ridge, Tennessee, USA
[4]Auburn University, Auburn, Alabama, USA
email: pomphrey@pppl.gov

Abstract.

The simulation of an entire NCSX discharge, the implications for plasma control, and work towards designing a set of magnetic diagnostics required to effect the necessary control are discussed. TRANSP is used to evolve the pressure and poloidal flux profiles in a 2D equivalent plasma model. Calculated profiles are input to STELLOPT to calculate the coil currents, 3D equilibrium, and constrained plasma physics properties. A set of magnetic diagnostics is being designed using a "control surface" and eigen-analysis database approach. Development of a stellarator equilibrium reconstruction tool V3FIT based on VMEC and EFIT are presented. Magnetic reciprocity relation is used to generalize the EFIT response function approach to 3D. Two tools, V3RFUN and V3POST, have been developed to efficiently compute 3D magnetic diagnostic responses and are being applied to support design of magnetic diagnostics. A prototype 3D reconstruction code for examination of numerical features of the reconstruction process has been built and is being tested.

1. Introduction and Motivation

The NCSX stellarator is a quasi-axisymmetric device under construction at PPPL. Operation and interpretation of experimental results will require accurate and efficient reconstruction of experimental equilibria and plasma control. The generation of substantial plasma current and the need to maintain kink stability and good quasi-axisymmetry throughout NCSX discharge evolution imposes greater shape control requirements than previous stellarators. In this paper, we discuss the simulation of an entire discharge, the implications for plasma control, and our work towards designing a set of magnetic diagnostics required to effect the necessary control. We also report recent progress in the development of a new stellarator equilibrium reconstruction tool, V3FIT. V3FIT is based on the widely used VMEC 3D equilibrium code and a 3D generalization of the efficient EFIT response function formalism that is extensively used in tokamak reconstruction.

Simulations for NCSX that evolve the plasma pressure and poloidal flux have recently been described by Lazarus et al [1]. Taking advantage of the quasi-axisymmetry of NCSX plasmas the pressure and poloidal flux profiles are evolved in an appropriately defined 2D "equivalent tokamak (ET)" using TRANSP [2]. The ET has the toroidally averaged plasma shape and plasma current with two distinct components: The first component is the usual plasma current in a tokamak, to be evolved by the transport model. The second is a fixed profile of 321 kA, modelled as lower hybrid current drive, that produces a rotational transform equal to the vacuum transform of NCSX. The transport model includes axisymmetric neoclassical diffusivities, a ripple diffusivity to account for the 3D magnetic field, and anomalous diffusivity in the electron and ion channels to make the total confinement time match the

maximum of neo-Alcator scaling [3] and ITER97L L-mode scaling [4]. The plasma current diffusion includes bootstrap current, flux from the Ohmic transformer, and neutral beam current drive. The neutral beams are balanced and to first order the neutral beam current drive is cancelled. However, because of different orbit losses for co- and counter-injection there is a residual. The ohmic current is programmed to initiate a plasma and then negate this residual so the bootstrap current, controlled by programming the neutral beam power and density, is the dominant term. The resulting pressure, p, and flux surface averaged toroidal current density, <J>, profiles are used in 3D, free boundary equilibrium calculations. As the p and <J> profiles evolve, appropriate modular and poloidal field coil currents are calculated using the STELLOPT optimization code [5] in two stages: First, currents are determined which produce a plasma with the same shape as the desired final β=4.0% reference configuration. The equilibria with the reference shape, but updated profiles do not generally preserve stability or quasi-symmetry. A second series of optimizations are performed to restore these features.

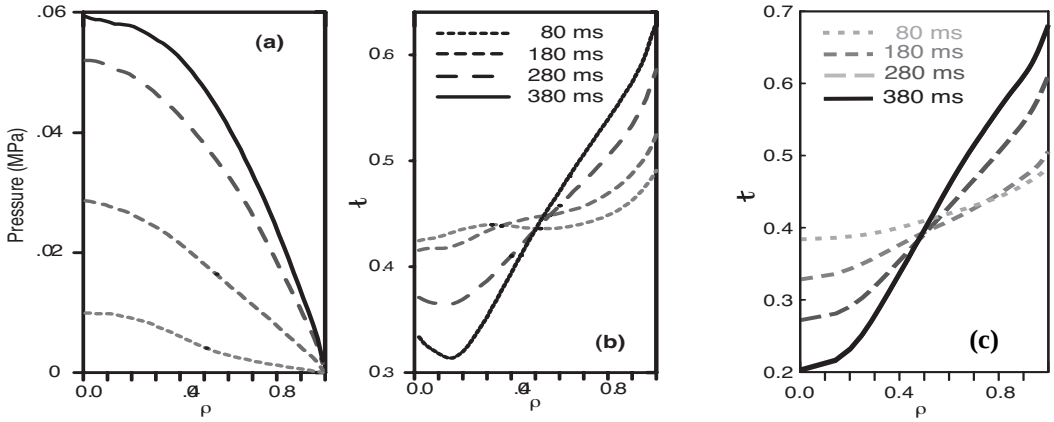

Figure 1. Plasma pressure and transform profiles at selected times from 2D simulation. (a) pressure profile, (b) transform resulting from 2D simulation, and (c) transform after 3D optimizations.

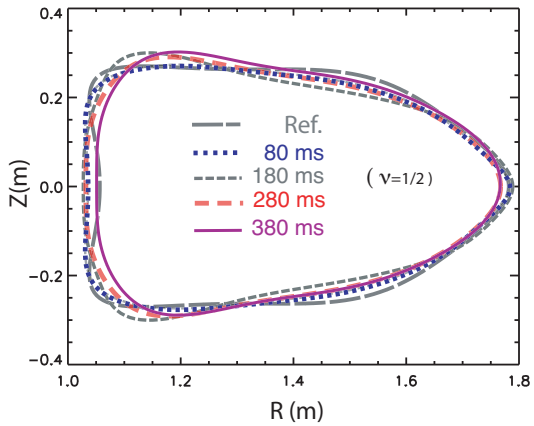

Figure 2. Plasma shapes in the ν=1/2 plane at times shown in Fig.1.

Plasma profiles at different stages of the simulation are shown in Fig. 1. In Fig. 1c it is seen that the optimizations change the plasma boundary in such a way as to strengthen the shear. The shape changes which restore quasi-symmetry and stability are shown in Fig.2.

2. Development of 3D Equilibrium Reconstruction for Compact Stellarators

Reconstruction of experimental equilibria has been an important part of tokamak data analysis and has contributed significantly to several major discoveries of tokamak physics. It is routinely used for shape control and to support plasma operation in tokamaks. Stellarators have now achieved significant β values and new hybrid stellarators such as NCSX, QPS, and CTH are designed to have a significant fraction of the rotational transform produced by plasma currents. Operation and interpretation of experimental results from these existing and new stellarators will require accurate and efficient reconstruction of experimental equilibria. In contrast to tokamaks, there is presently only a limited capability to reconstruct experimental equilibria from magnetic signals in stellarators.

In this Section, recent progress in the development of a new 3D equilibrium reconstruction tool, V3FIT, is presented. V3FIT is based on the widely used VMEC 3D equilibrium code [6] and the efficient EFIT response function formulism that is extensively used in tokamak reconstruction [7]. The goal for the V3FIT project is to develop a 3D equilibrium reconstruction code as helpful for stellarators as EFIT is for tokamaks. Although the primary intention for V3FIT is for stellarator applications, it will also be useful for investigation of 3D error field effects on experimentally reconstructed equilibrium in tokamaks

A key step towards the development of V3FIT is the generalization of the EFIT response function method to 3D magnetic geometry. This allows the lengthy calculations of the inductance matrix to be pre-computed, stored, and separated from the rapid calculations of magnetic signals. Using the magnetic reciprocity relation, a 3D response function approach has been formulated that allows the plasma contribution to the magnetic flux $\boldsymbol{\psi}^{\mathbf{i}}_{\mathbf{plasma}}$ through the i^{th} diagnostic loop to be directly related to the plasma current distribution in term of a response potential for the diagnostic loop, $\mathbf{a}^{\mathbf{i}}_{\mathbf{diag}}$, and an integration over the plasma volume [8]

$$\psi^{i}_{plasma} = \int_{V_P} dV' J_{plasma}(x') \bullet a^{i}_{diag} \,. \qquad (1)$$

Here, $\mathbf{J}_{\mathrm{plasma}}$ is the plasma current density. The response potential $\mathbf{a}^{\mathbf{i}}_{\mathbf{diag}}$ depends only on the geometry of the diagnostic itself and can be conveniently pre-computed and stored. The volume integration can be converted to a surface integration using the virtual casing principle. When the detailed dependence on internal plasma profiles is not needed and only the net plasma-induced flux response is required, the surface form is more useful and generally computationally more efficient than the volume integral.

Two computational tools, V3RFUN and V3FIT, have been developed to efficiently compute 3D magnetic responses to a diagnostic set based on this new response function approach [8]. V3RFUN computes the diagnostic response functions from the plasma and the external coils and stores them in separate files, which can be subsequently retrieved and used to efficiently compute the magnetic responses for arbitrary equilibria. The computation of the response function is done using the recently analytically derived compact expression for the magnetic vector potential of a current line segment [9]. These expressions, together with the efficient use of Fortran modularization, leads to reduction of nearly a factor of 2 in the time to numerically evaluate the 3D diagnostic responses for stellarators.

V3FIT reads the pre-stored response functions and efficiently computes the magnetic response to a diagnostic set for an arbitrary equilibrium. To evaluate the plasma contribution to the magnetic responses using either the volume or the surface integration approach, values of the response functions stored in the database are interpolated onto the flux coordinate grid. The database is constructed to store response functions at each toroidal plane required to numerically compute the integral. Therefore, only 2D interpolation is required, which is done using the 4-point bilinear formula and is extremely fast. Together with the fact that the data retrieval process comprises a small fraction of the time to generate the database values, this makes the present method to calculate the magnetic response computationally very efficient.

Comparative calculations for various stellarator and tokamak diagnostics using the present database approach have been carried out against calculations from other codes. The results from V3RFUN and V3POST are in good agreement with those from other codes. This is illustrated in Table 1, where the plasma contributions to a set of W7-AS magnetic diagnostic computed using V3RFUN/V3POST are compared to those computed using the DIAGNO code. In this case, the V3POST results are computed using the volume form, whereas the DIAGNO results are computed using the surface form. The relative discrepancy is quite small. The CPU time used by V3POST to compute these magnetic responses is ~ 2% of that used to generate the response function database and ~ 0.9% of that used to compute the equilibrium. Thus, the database approach is an efficient numerical scheme for computing the diagnostic fluxes in a stellarator plasma and will be very useful for diagnostic development and reconstruction applications. The V3RFUN/V3POST results have also been compared to those computed using the MFBE code and good agreements are obtained. V3RFUN/V3POST is being applied to support design of magnetic diagnostics for NCSX and CTH.

	Outer MP	Inner MP	Loop 3	Mod Loop 2	Loop 1	Diam1-New	Diam2
DIAGNO	-12.43	7.583	-1.030	-0.7319	0.6479	0.6041	0.5615
V3POST	-12.48	7.676	-1.032	-0.7324	0.6484	0.6022	0.5594
Rel. Diff (%)	0.37	1.21	0.19	0.067	0.080	0.32	0.38

TABLE 1. COMPARISON OF PREDICTED FLUX SIGNALS IN mWb FOR W7-AS

Both V3RFUN and V3POST have been incorporated into the 3D stellarator optimization code STELLOPT to provide a prototype 3D reconstruction code that can be used to examine various numerical features of the reconstruction process, such as the level of convergence needed to estimate the signal gradients, and to guide the development of the optimized V3FIT code. STELLOPT employs the Levenberg-Marquardt quasi-global minimization method to search for the optimum state vector. The method requires a large number of equilibrium calculations to compute the signal gradients used to guide the search. Although it is computationally intensive and slow, this proto-type code is useful for testing the efficiency of various algorithms to compute the gradient vector.

Various linearization schemes to approximate the signal gradients and to speed up the search process based on the efficient 2D EFIT optimization scheme have also been formulated. Unlike the 2D toroidally axisymmetric case, in 3D the magnetic flux is related to the current source in a more complex way that involves both the poloidal and the toroidal components of the current density. These are linearized by eliminating one of them in terms of the other using the pressure balance equation plus a Picard iteration scheme.

3. Magnetic Measurements: Information Content and Diagnostics Selection

A variety of external magnetic diagnostics (MD's) will be installed on NCSX and used for real-time plasma shape control and between-shot equilibrium reconstruction. The set will include diamagnetic loops, Rogowski coils, and flux loops wound on the modular and poloidal field coils. Additionally, there will be some number (to be determined) of triple-axis magnetic probes, poloidal and toroidal flux loops on the vacuum vessel, saddle coils arrayed on the vacuum vessel surface, and saddle coils at port penetrations of the structural shell. We are presently focused on determining a minimum set of diagnostics adequate for the task. Our criterion for sufficiency of the diagnostic set will be a demonstrated ability to "reconstruct" the magnetic fields produced by a database (currently > 500) of VMEC free-boundary equilibria. The equilibria encompass the range of plasma conditions (currents, fields, shapes and β) that can be expected to be produced in the device and incorporate random combinations of 28 current profiles and 22 pressure profiles. Equilibria are neither constrained to be kink and ballooning stable, nor optimized with respect to quasi-

axisymmetry. Magnetic field components due to each equilibrium are calculated on a uniform mesh on a single toroidal "control surface" (CS) placed 1 cm outside the envelope of all equilibria. For the diagnostics selection calculations, reconstruction is defined as the ability to accurately predict the component field patterns produced on the CS using the magnetic diagnostic signals. For a given set of diagnostics, reconstruction is a linear problem amenable to matrix analysis.

Field patterns for the ensemble of equilibria are conveniently described using Empirical Orthogonal Functions (EOFs) [10]: For each equilibrium, labelled by index j, we calculate the poloidal component of B, B_θ, at each point on the CS mesh with the mean signal (over the ensemble) subtracted off . The signal is stored as an M-element column vector x_j. Data from N equilibria naturally form an MxN matrix, X, whose Singular Value Decomposition (SVD) is $X = U\ W\ V^T$. Here, U and V are MxM and NxN unitary matrices and W is an MxN diagonal matrix. Each column of X is given, exactly, as a linear combination of r = min(M,N) columns of U: $\mathbf{x}_j = \Sigma_{k=1\rightarrow r}\{p_k(j)\mathbf{u}_k\}$, where $p_k(j) \equiv V_{jk}w_k$ and EOF $\mathbf{u}_k$ is the kth column of U. Truncation of the sum at $k = k_{max} < r$ leads to a "best" approximation $\mathbf{x}_j^{kmax}$ to $\mathbf{x}_j$ (minimizes $||\mathbf{x}_j - \mathbf{x}_j^{kmax}||$). The $\mathbf{u}_k$ are eigenfunctions of the covariance matrix XX^T with eigenvalues w_k^2 equal to the square of the singular values of X (diagonal entries of W). Columns of V are eigenfunctions of X^TX. Each $\mathbf{u}_k$ is an independent field pattern on the CS whose contribution to the variance of the database signals is given by w_k^2. Small eigenvalues correspond to insignificant field patterns [11].

Figures 3a and 3b shows the singular value spectrum for the plasma contribution to B_θ on the CS. The present NCSX database with N=504 equilibria was used, with B_θ calculated at M=1200 points in one field period of the CS . The first 20 singular values are shown. Only 4 magnetic field patterns are significant, contributing 78.9%, 19.5%, 0.6% and 0.4%, for a total of 99.4%, of the variance in the field measured on the control surface. Previously reported SVD calculations by Callaghan et al., [10] for W7-AS show similar results.

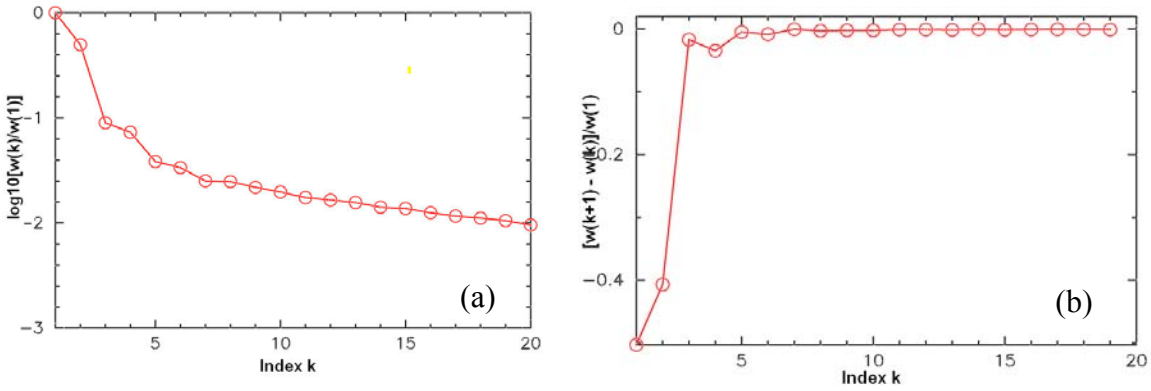

Figure 3. Singular value decomposition of B_θ field patterns on CS.
(a) Logarithmic scree plot of singular values vs pattern index k. (b) Incremental change in the singular values - shows convergence if 4 singular values are retained.

The interpretation of the four dominant field patterns, $\mathbf{u}_{1\text{-}4}$, is presently unclear; however the columns of V provide partial understanding: Each row of X can be written in terms of the columns of V as $(\mathbf{x}^i)^T = \Sigma_{k=1\rightarrow r}\{q_k(i)\ \mathbf{v}_k\}$, where $q_k(i) = U_{ik}w_k$. The ith component of $\mathbf{v}_k$, V_{ik}, is therefore a measure of the contribution of the ith equilibrium to the kth magnetic field pattern $\mathbf{u}_k$. For ease of illustration consider N=5 equilibria from the database. Current and pressure profile combinations in the subset are {(J1, P1), (J2, P1), (J3, P1), (J1, P2), (J1, P3)} where J1-3 and P1-3 are shown in Fig. 4. Each of the five equilibria has the same total plasma current, toroidal field and β. SVD analysis of this reduced database yields four non-zero singular values (subtracting the mean of the B_θ signals from each point on the CS leads to a zero eigenvalue), and four corresponding field patterns. The variance contributions are 71.3%, 21.5%, 7.0% and 0.2%, respectively (similar, by coincidence, to the variance

contributions of the dominant 4 patterns of the full database). The $\mathbf{v}_k$ vectors corresponding to each of $\mathbf{u}_{1\text{-}4}$ are tabulated in Table 2.

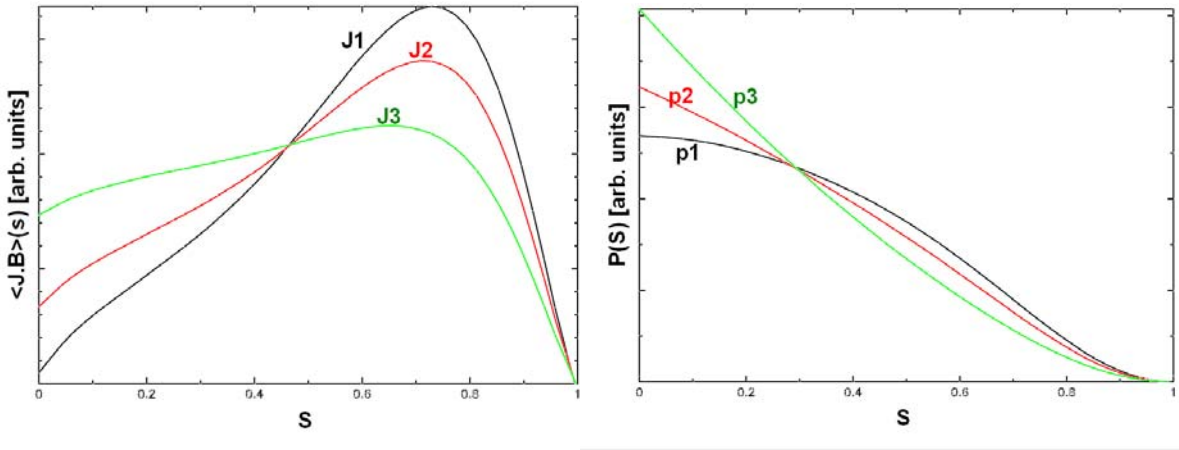

Figure 4. Profiles of current and pressure, combinations of which define the reduced database of 5 equilibria used to illustrate the interpretation of field patterns.

$\mathbf{v}_1$=Col$_1$(V)	$\mathbf{v}_2$=Col$_2$(V)	$\mathbf{v}_3$=Col$_3$(V)	$\mathbf{v}_4$=Col$_4$(V)
+0.1	-0.2	+0.4	-0.8
-0.5	+0.5	+0.5	+0.3
-0.6	-0.3	-0.6	-0.1
+0.4	-0.6	+0.2	+0.6
+0.5	+0.6	-0.4	-0.1

TABLE 2. FIRST FOUR COLUMNS ($\mathbf{v}_{1\text{-}4}$) OF V FOR REDUCED DATABASE.

Entries in rows 2 and 3 of the first column of V have similar magnitude but opposite sign to the entries in rows 4 and 5. This sign and relative magnitude show that the field pattern accounting for >70% of the variance in the data distinguishes between variations in current profile and pressure profile (see [12] for related work). The remaining patterns represent contrasts within the separate scans. Examination of the columns of V for the full NCSX database of equilibria shows that the dominant field pattern has $V_{i,k=1}$ components all with the same sign. This indicates a measure of overall size of some feature shared by the equilibria. We speculate this feature is the stored energy, present in the full database but absent in the reduced database. The second field pattern shows a similar contrast of signs to the first pattern of the reduced database. Since EOF field patterns are constructed to be orthogonal, we should not expect any single pattern to correspond to the variation of a single familiar physics parameter, such as β_{pol} or ℓ_i. Interpretation of the EOF patterns is not essential for magnetic diagnostics design. However it is desirable that whatever diagnostics set is finally chosen for NCSX should be capable of resolving all $\mathbf{u}_{1\text{-}4}$.

Figure 5 shows a subset of candidate diagnostics for NCSX in the form of saddle flux loops wound at port penetrations of one field period sector of the vacuum vessel, and triple-axis B-probes equally spaced on a Fourier surface 2 cm within the vacuum vessel surface, and shown in an adjacent field period for ease of viewing. The saddle loops, numbered 1-15 for reference below, are in locations compatible with hardware constraints. When the time comes to make the final choice for number and position of diagnostics it will be useful to have some understanding of which, among candidate sets such as those shown, provide the most useful

information. Below, we discuss SVD methods for ranking diagnostics. The exposition focuses on the saddle loops.

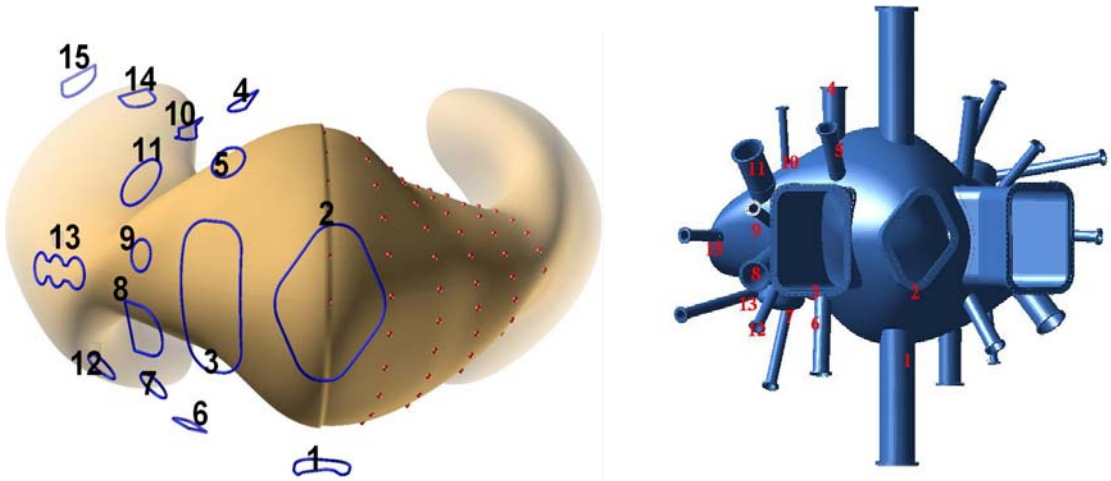

Figure 5. Candidate diagnostics for NCSX: (a) 15 saddle flux loops (blue) at port penetrations of one period of the vacuum vessel, and triple-axis B-probes (red) equally spaced on Fourier surface 2.0 cm inside vacuum vessel surface. (b) Vacuum vessel structure showing port penetrations.

Signal values from the M=15 saddle loops for the N=504 equilibria are stored as column vectors $\mathbf{x}_i$ of matrix X. After SVD calculation of X an appropriate cutoff for the singular value spectrum is chosen so that m EOFs account for some acceptable value for the cumulative variance. Then L=M-m diagnostics are potential candidates for rejection. Beginning with EOF $\mathbf{u}_j$ whose eigenvalue (labelled by j) is smallest, we identify that diagnostic (labelled by i) whose $|U_{ij}|$ is largest. Diagnostic i becomes the primary candidate for rejection. The procedure is repeated, in succession, for j = M→m+1 rejecting at each step that i-labelled diagnostic for which $|U_{ij}|$ is maximum, and which has not previously been rejected. The rationale for the rejection method, known in multivariate statistics as Jolliffe's B2 method [11], is that if M diagnostics provide only m<M independent measurements then L = M-m linear dependencies exist of the form $\mathbf{c}_i \bullet \mathbf{x}_i = 0$ where the $\mathbf{c}_i$ are constant vectors. SVD detects such linear dependencies: $U^T X = WV^T \Rightarrow \mathbf{u}_i \bullet \mathbf{x}_j = w_i V_{ji}$ so that if singular value w_i is sufficiently small to be considered zero then $\mathbf{u}_i \bullet \mathbf{x}_j = 0$ for all j. Therefore the components of $\mathbf{u}_i$ are the same coefficients as those which express the linear dependencies within the diagnostics set (i.e., $\mathbf{u}_i \equiv \mathbf{c}_i$ above). An EOF with $w_i = 0$ satisfies $U_{1i}X_{1j} + U_{2i}X_{2j} + ... + U_{ki}X_{kj} + ... = 0$ so that any one of the X_{kj} for which $U_{ki} \neq 0$ can be expressed as a linear combination of all other X_{mj} for which $U_{mi} \neq 0$. The k-labelled diagnostic is therefore redundant. Choosing k for which $|U_{ki}|$ is maximum provides indentification of the redundant variable.

Table 3 tabulates the saddle port EOF components $U_{i=1\rightarrow 15,j}$ for each of the five smallest singular values (i.e., j=11-15). Following the discussion in the previous paragraph, a ranking list for the least important port saddles is: i=2, 13, 6 or 14, 9, 5. A modest extension of Jolliffe's B2 method involves re-computing the SVD of X after eliminating each diagnostic. The result of such a calculation is tabulated in Table 4, where each row shows the saddle port EOF corresponding to the smallest singular value. The ranking list through five eliminations is i=2, 13, 6, 9, 10 and differs from the single SVD calculation B2 scheme only in the choice of the 5th member of the list.

$\mathbf{u}_{15}^T$	+0.0	-0.9	+0.0	+0.0	-0.0	+0.0	+0.0	-0.0	-0.0	+0.0	+0.0	+0.0	-0.5	+0.0	+0.0
$\mathbf{u}_{14}^T$	-0.0	-0.5	-0.0	-0.0	+0.0	+0.0	-0.0	+0.0	+0.0	-0.0	-0.0	-0.0	+0.9	+0.0	-0.0
$\mathbf{u}_{13}^T$	+0.0	-0.1	-0.0	-0.0	+0.0	-0.7	-0.0	+0.0	+0.0	-0.0	+0.0	-0.0	+0.0	-0.7	-0.0
$\mathbf{u}_{12}^T$	+0.0	-0.0	-0.0	-0.0	+0.2	-0.0	+0.5	-0.1	-0.7	-0.2	-0.2	+0.2	+0.0	+0.0	+0.1
$\mathbf{u}_{11}^T$	+0.0	-0.0	+0.1	+0.1	-0.8	+0.1	+0.1	-0.2	-0.2	+0.0	+0.2	-0.2	+0.0	-0.1	+0.4

TABLE 3. SADDLE PORT EOFs, $\mathbf{u}_{11\text{-}15}$ FOR SMALLEST 5 SINGULAR VALUES. ONLY 1 SIGNIFICANT FIGURE IS SHOWN.

$\mathbf{u}_{15}^T$	+0.0	-0.9	+0.0	+0.0	-0.0	+0.0	+0.0	-0.0	-0.0	+0.0	+0.0	+0.0	-0.5	+0.0	+0.0
$\mathbf{u}_{14}^T$	-0.0	X	-0.0	-0.0	+0.0	+0.0	-0.0	+0.0	+0.0	-0.0	-0.0	-0.0	+1.0	+0.0	-0.0
$\mathbf{u}_{13}^T$	-0.0	X	+0.0	+0.0	-0.0	+0.7	+0.0	-0.0	-0.0	+0.0	-0.0	+0.0	X	+0.7	+0.0
$\mathbf{u}_{12}^T$	-0.0	X	+0.0	+0.0	-0.3	X	-0.5	+0.1	+0.7	+0.2	+0.2	-0.2	X	-0.0	-0.1
$\mathbf{u}_{11}^T$	-0.0	X	+0.0	+0.0	-0.3	X	-0.5	+0.1	X	+0.7	+0.2	+0.2	X	-0.1	-0.1

TABLE 4. SADDLE PORT EOFs FOR SMALLEST SINGULAR VALUE WHEN SVD IS RE-COMPUTED AFTER ELIMINATION OF EACH DIAGNOSTIC.

Calculations for testing the reconstruction of equilibrium fields on the CS for different numbers of diagnostics will make use of the selection techniques discussed above. Once a set is found which adequately reproduces the CS field patterns, we will need to perform actual equilibrium reconstructions to assure ourselves we do have the information necessary for plasma control. Additional diagnostics need to be incorporated to measure deviations from stellarator symmetry. Diagnostics sensitive to error fields generated by eddy currents flowing in the vacuum vessel structure will also be added.

Acknowledgment

The work discussed in this paper was supported by U.S. Department of Energy under Contract No. DE-AC02-76CH03073 and Grants DE-FG03-95ER54309, DE-FG02-03ER54692, DE-FG02-00ER54610.

References

[1] E.A. LAZARUS, et al., Fusion Science & Tech. **46** (2004) 213.
[2] R.V.BUDNY, D.R.ERNST, T.-S.HAHM, et al., Physics of Plasmas **7** (2000) 5038.
[3] R.R. PARKER, Nuc. Fusion **25** (1985) 1127.
[4] S. KAYE, et al., Nuc. Fusion 37 (1997) 1303.
[5] D.J. STRICKLER, et al., Fusion Science & Tech. **45** (2004) 15.
[6] S.P. HIRSHMAN AND J.C. WHITSON, Phys. Fluids **26** (1983) 3553.
[7] L.L. LAO, et al., Nuc. Fusion **25** (1985) 1611
[8] S.P. HIRSHMAN, E.A. LAZARUS, J.D. HANSON, S.F. KNOWLTON, L.L. LAO, Phys. Plasmas **11** (2004) 595.
[9] J.D. HANSON, S.P. HIRSHMAN, Phys. Plasmas **9** (2002) 4410.
[10] H.P. CALLAGHAN, P.J. McCARTHY, J. GEIGER, 27th EPS Conference on Contr. Fusion and Plasma Phys. Budapest 12-16 June 2000. ECA Vol. **24B** (2000) 436.
[11] I.T. JOLLIFFE, Principal Component Analysis, Springer-Verlag (2002).
[12] M.C. ZARNSTORFF, "Equilibrium and Stability of High Beta Plasmas in W7-AS, Paper EX/3-4, these Proceedings.